© 2016. Published by The Company of Biologists Ltd | Journal of Cell Science (2016) 129, 2686 doi:10.1242/jcs.193615

RETRACTION

Retraction: GRIM-19-mediated translocation of STAT3 to mitochondria is necessary for TNF-induced necroptosis

Nataly Shulga and John G. Pastorino

Retraction of: *J. Cell Sci.* **125**, 2995-3003

This article has been retracted at the request of the corresponding author, John G. Pastorino.

This notice updates and replaces a recent Expression of Concern, published on 15 February 2016.

Journal of Cell Science was alerted to potential blot duplication and reuse in the following five papers published in Journal of Cell Science by John G. Pastorino:

Sirtuin-3 deacetylation of cyclophilin D induces dissociation of hexokinase II from the mitochondria
Nataly Shulga, Robin Wilson-Smith and John G. Pastorino
J. Cell. Sci. (2010) **123**, 894-902

Ethanol sensitizes mitochondria to the permeability transition by inhibiting deacetylation of cyclophilin-D mediated by sirtuin-3
Nataly Shulga and John G. Pastorino
J. Cell. Sci. (2010) **123**, 4117-4127

GRIM-19-mediated translocation of STAT3 to mitochondria is necessary for TNF-induced necroptosis
Nataly Shulga and John G. Pastorino
J. Cell. Sci. (2012) **125**, 2995-3003

Sirtuin-3 modulates Bak- and Bax-dependent apoptosis
Manish Verma, Nataly Shulga and John G. Pastorino
J. Cell. Sci. (2013) **126**, 274-288

Mitoneet mediates TNFα-induced necroptosis promoted by exposure to fructose and ethanol
Nataly Shulga and John G. Pastorino
J. Cell. Sci. (2014) **127**, 896-907

These concerns were relayed to Dr Pastorino, the corresponding author, who responded with an explanation and original data. Following review of these data, we felt unable to resolve this matter at a distance, so contacted the authors' institution (Rowan University) and requested that they investigate further.

Following their assessment, Rowan University required that Dr Pastorino retract all of the above named papers published in Journal of Cell Science. Dr Pastorino also entered a Voluntary Exclusion Agreement with The Office of Research Integrity (ORI); the agreement can be found here: http://ori.hhs.gov/content/case-summary-pastorino-john-g.

ORI found that Dr Pastorino intentionally falsified and/or fabricated data and, specifically, that he "duplicated images, or trimmed and/or manipulated blot images from unrelated sources to obscure their origin, and relabelled them to represent different experimental results in:"

- Figures 2A,C; 3B; 5A; 7B; 8A in *J. Cell. Sci.* (2010a), **123**, 894-902.
- Figures 2B; 5A; 6A,B in *J. Cell. Sci.* (2010b), **123**, 4117-4127.
- Figures 1A; 2A,B; 4C; 5A,B; 6A; 7A–C in *J. Cell. Sci.* (2012) **125**, 2995-3003.
- Figures 4F; 5H; 6A in *J. Cell. Sci.* (2013) **126**, 274-288.
- Figures 1B; 2B,C; 3A,B; 4D in *J. Cell. Sci.*(2014) **127**, 896-907.

GRIM-19-mediated translocation of STAT3 to mitochondria is necessary for TNF-induced necroptosis

Nataly Shulga and John G. Pastorino*

Department of Molecular Biology, School of Osteopathic Medicine, University of Medicine and Dentistry of New Jersey, Stratford, New Jersey 08084, USA

*Author for correspondence (pastorjg@umdnj.edu)

Accepted 8 February 2012
Journal of Cell Science 125, 2995–3003

doi: 10.1242/jcs.103093

Summary

Tumor necrosis factor (TNF) can induce necroptosis, wherein inhibition of caspase activity prevents apoptosis but initiates an alternative programmed necrosis. The activity of receptor-interacting serine/threonine-protein kinase 1 (RIPK-1) is required for necroptosis to proceed, with suppression of RIPK-1 expression or inhibition of RIPK-1 activity with necrostatin-1 preventing TNF-induced necroptosis. Downstream from the TNF receptor, the generation of reactive oxygen species at the mitochondria has been identified as necessary for the execution of necroptosis; with antioxidants and inhibitors of mitochondrial complex I preventing TNF-induced cytotoxicity. However, components of the signaling pathway that lie between activated RIPK-1 and the mitochondria are unknown. In the study reported here we demonstrate that during TNF-induced necroptosis, STAT3 is phosphorylated on serine 727 which is dependent on RIPK-1 expression or activity. The phosphorylation of STAT3 induces interaction with GRIM-19, a subunit of mitochondrial complex I, with a resultant translocation of STAT3 to the mitochondria, where it induces an increase in reactive oxygen species production and cell death.

Key words: TNF, STAT3, GRIM-19, Necroptosis, Mitochondria

Introduction

Tumor necrosis factor α (TNF) is a cytokine with a myriad of effects on varied cell types including adipocytes, osteocytes and immune cells. However, its most studied and dramatic effect is cell death. TNF does this by engaging TNF receptor 1 (TNFR1), which is the only TNF receptor capable of initiating apoptosis or necroptosis. TNF binding to TNFR causes receptor trimerization and the formation of an intracellular death-inducing signaling complex (DISC) (Ganten et al., 2004; Kim et al., 2000). The intracellular signaling network initiated by TNF is remarkably diverse and can result in the stimulation of survival pathways such as that mediated by NF-κB or in the initiation of caspase activity. Pro-caspase-8 is recruited to the DISC where it exhibits proximity-induced activation (Ganten et al., 2004; Kuwana et al., 1998; Zhuang et al., 1999). In turn, caspase-8 can cleave and activate effector caspases such as caspase-3 that promulgate the apoptotic cascade. Inhibition of caspase-8 activity prevents TNF-induced apoptosis. However, in some cell types, inhibition of caspase-8 leads to an alternative pathway that terminates in necrotic cell death (Vercammen et al., 1998). The programmed necrosis brought about by TNF has been termed necroptosis. The enzymatic activity of receptor-interacting serine/threonine-protein kinase 1 (RIPK-1) is required for necroptosis. The internalization of the TNFR leads to the assembly of a complex that includes TRADD, FADD, caspase- 8, RIPK-3 and RIPK-1, termed complex II. Remarkably, activated caspase-8 cleaves and inactivates RIPK-1 and 3, eventuating in apoptosis (Oberst et al., 2011). However, when caspase-8 is absent or inactivated, RIPK-1 and RIPK-3 become active in what has been termed a necrosome (Galluzzi et al., 2011; Vandenabeele et al., 2010; Vanlangenakker et al., 2011; Wallach et al., 2011). RIPK-3 phosphorylates and stimulates the activity of RIPK-1, stabilizing the pro-necrotic RIPK-1–RIPK-3 complex (Cho et al., 2009). In turn, RIPK-1 activity is required for RIPK-3 phosphorylation and the necrotic activity of the necrosome, with inhibition of RIPK-1 by necrostatin-1 preventing necroptosis.

Inhibition of reactive oxygen species (ROS) production with antioxidants prevents TNF-induced necroptotic cell death (Goossens et al., 1995; Schulze-Osthoff et al., 1992). The RIPK-1–RIPK-3 necrosome triggers the increased production of ROS that characterizes and precedes TNF-induced cytotoxicity (Kasof et al., 2000; Lin et al., 2004; Zhang et al., 2009). There is evidence that mitochondrial energy metabolism is the source of necrosome-induced ROS formation. The necrosome stimulates the activities of glycogen phosphorylase and glutamate dehydrogenase, the products of which feed into the Krebs cycle and ultimately the mitochondrial respiratory chain. Components of the mitochondrial respiratory chain have been shown to be a source of ROS, with complex I being a particularly active producer of ROS under some circumstances. Indeed, site-specific inhibitors of complex I such as rotenone and amytal prevent TNF-induced cytotoxicity (Schulze-Osthoff et al., 1992).

STAT3 is localized to the cytosol and can translocate to the nucleus, where it is a transcriptional regulator (Demaria et al., 2010; Demaria and Poli, 2011). However, recent studies indicate that STAT3 is also localized to the mitochondria (Gough et al., 2009; Wegrzyn et al., 2009). In particular, phosphorylation of STAT3 on tyrosine 705 promotes its translocation to the nucleus, whereas phosphorylation on serine 727 is associated with a mitochondrial localization. Mitochondrial STAT3 increases the activity of complexes I and II of the respiratory chain in a transcription-independent manner. However, without a

mitochondrial localization sequence, the mechanism by which STAT3 transits from the cytosol to the mitochondria is unclear. GRIM-19 (also known as NADH dehydrogenase [ubiquinone] 1 alpha subcomplex subunit 13; encoded by *Ndufa13*) is a component of complex I of the mitochondrial respiratory chain (Fearnley et al., 2001). Suppression of GRIM-19 reduced ROS formation and cell death induced by interferon-β and retinoic acid treatment (Huang et al., 2007). GRIM-19 interacts with STAT3, with serine727 of STAT3 being necessary for the GRIM-19–STAT3 interaction (Zhang et al., 2003). Like STAT3, GRIM-19 is also found in the mitochondria, cytosol and nucleus and is capable of translocating from one site to another upon stimulation by cytokines. In the study reported here we demonstrate that during TNF-induced necroptosis, STAT3 undergoes phosphorylation on serine727 that is dependent on RIPK-1 expression and activity. Upon phosphorylation of serine727, STAT3 interacts with GRIM-19, which brings about accumulation of STAT3 and GRIM-19 in the mitochondria, where they induce an increase in ROS production and cell death by necroptosis.

Results

Suppression of STAT3 expression inhibits TNFα-induced ROS generation and necroptosis

STAT3 expression was suppressed in L929 mouse fibrosarcoma cells using siRNA targeting STAT3. As seen in Fig. 1A, transfection of *Stat3* siRNA greatly suppressed the expression of STAT3 while having little effect on the levels of STAT1. By contrast, siRNA targeting STAT1 had no effect on STAT3 expression but suppressed expression of STAT1. TNF in the presence of the pan caspase inhibitor, Z-VAD-FMK (ZVAD), known to induce necroptosis in L929 cells. As shown in Fig. 1B (left panel), L929 cells transfected with non-targeting siRNA displayed an extensive loss of cell viability when exposed to TNFα in the presence of ZVAD, with only 12% of the cells viable after 18 hours of exposure. By contrast, suppression of STAT3 expression prevented TNFα-induced necroptosis, with cell viability remaining at 88% after 18 hours of exposure (Fig. 1B, left panel). Notably, suppression of STAT1 expression did not prevent TNF+ZVAD-induced necroptosis, with only 12% of the cells remaining viable after 18 hours of exposure (Fig. 1B, left panel).

TNF-induced necroptosis is mediated in part by ROS generated by mitochondria. MitoSOX is a potentiometric dye that localizes to the mitochondria and exhibits an increase in fluorescence when oxidized by superoxide anions generated by the mitochondrial electron transport chain. As shown in Fig. 1B, right panel, treatment with TNF+ZVAD induced a marked increase in MitoSOX fluorescence that was not prevented by transfection with non-targeting siRNA or siRNA against STAT1. Notably, the peak in ROS production occurred 4 hours after TNF+ZVAD addition, a time that precedes any appreciable loss of cell viability. By contrast, suppression of STAT3 expression completely prevented TNF+ZVAD-induced ROS formation, with MitoSOX fluorescence the same as that of control non-treated cells (Fig. 1B, right panel).

Phosphorylation of STAT3 on serine 727 is required for ROS generation and cytotoxicity during TNF-induced necroptosis

STAT3 is phosphorylated on many residues with tyrosine 705 and serine 727 being the best characterized. As shown in Fig. 2A, in untreated cells, there was a low level of STAT3

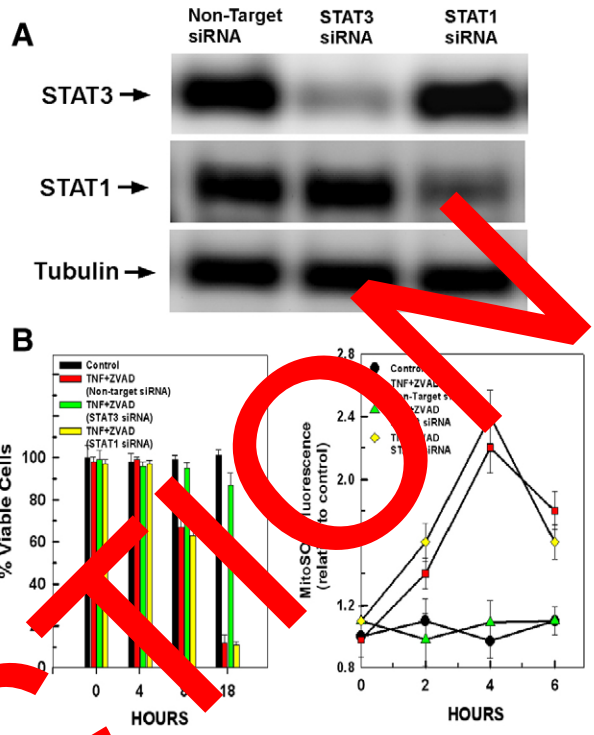

Fig. 1. STAT3 expression is necessary for ROS generation and cytotoxicity during TNF-induced necroptosis. (**A**) L929 cells were transfected with 50 nM siRNA targeting STAT3, STAT1 or a non-targeting control siRNA. Following 48 hours incubation, the cells were harvested and the levels of STAT3 and STAT1 were determined by western blotting. The blots were then stripped and reprobed with an antibody against tubulin. The results are typical of three independent experiments. (**B**) L929 cells were transfected with 50 nM non-targeting control siRNA or siRNAs targeting STAT3 or STAT1. Following 48 hours incubation, the cells were treated with 20 ng/ml TNFα in the presence of the pan-caspase inhibitor Z-VAD-FMK (ZVAD; 20 μM). At the time points indicated, the cells were harvested and their viability or generation of mitochondrial superoxide anion production was determined using propidium iodide and MitoSOX red, respectively, as described in the Materials and Methods. Values are the means of three independent experiments with the error bars indicating standard deviations.

phosphorylation on both tyrosine 705 and serine 727. Treatment of the cells with TNF alone for 4 hours did not stimulate phosphorylation of STAT3 on tyrosine 705 or serine 727 (Fig. 2A, lane 2). Likewise, treatment with ZVAD alone for 4 hours did not stimulate STAT3 phosphorylation on either residue (Fig. 2A, lane 3). However, exposure of the cells to TNF in the presence of ZVAD for 4 hours induced a marked increase in STAT3 phosphorylation on serine 727, while having little effect on the phosphorylation of tyrosine 705 (Fig. 2A, lane 4). As shown in Fig. 2B, the TNF+ZVAD-induced phosphorylation of STAT3 on serine 727 was first detectable at 30 minutes and became maximal by 4 hours of exposure, with no detectable change in STAT3 expression (less than 10% variation, according to densitometry).

We next wanted to determine the importance of TNF+ZVAD-induced phosphorylation of STAT3 for ROS production and cytotoxicity. L929 cells were generated with doxycycline inducible expression of non-phosphorylatable forms of STAT3 mutated at serine (S) 727 or tyrosine (Y) 705 to determine their effects on TNF-induced necrosis. Doxycycline induced the

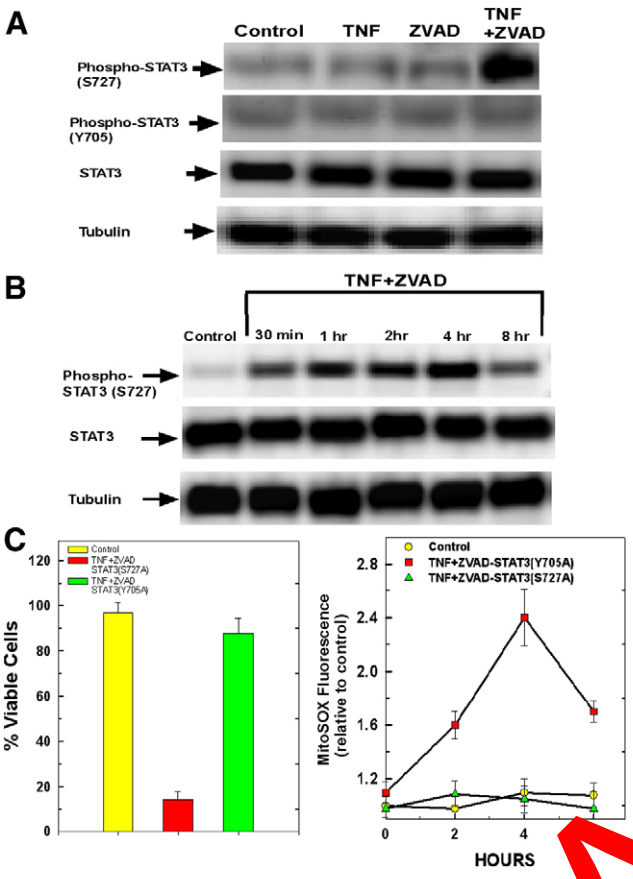

Fig. 2. STAT3 is phosphorylated on serine 727 during TNF-induc necroptosis and is required for ROS generation and xicity. (**A**) L929 cells were either left untreated or treated n 20 n l TNF, 20 μM ZVAD or a combination of TNF and ZVA After 4 ho s incubati the cells were harvested. Whole-cell extracts w prepared SDS-PAGE, then transferred to PVDF membran The ots re probed w antibodies specific for STAT3 phospho ted on tyr e 705 or serine 727. The blots were then stripped and rep d with antibod against total STAT3 and tubulin. The results a repr tative of three dependent experiments. (**B**) L929 cells were reated wi 0 ng/ml TNFα in combination with 20 μM ZVAD. At the t e points indicate e cells were harvested and whole-cell extracts prep d. The extracts were se ted by SDS-PAGE and then transferred to PV membra s for western blotting. The membranes were probed with a tibody a nst STAT3 phosphorylated on serine 727, then stripped and repr d w antibodies gainst total STAT3 and tubulin. The results a epresenta of three i pendent experiments. (**C**) L929 cells wer enera for tetr line ducible expression of STAT3 S727A or ST 5 T705A. e cells we ed in 24-well plates at 40,000 cells/well. Fol ing 24 ho of induction with 1 μg/ml doxycycline, the cells were treate ith 2 g/ml TN combination with 20 μM ZVAD. At the time points in d, the cells were harvested and cell viability and ROS formation w assessed using propidium iodide and MitoSOX, respectively. Values are the ns of three independent experiments with the error bars indicating standard deviations.

expression of FLAG-tagged STAT3 Y705A and STAT3 S727A at 24 hours (supplementary material Fig. S1). As shown in Fig. 2C, left panel, inducible expression of STAT3 Y705A provided no protection against TNF+ZVAD-induced necrosis, with only 14% of the cells viable after 18 hours of exposure. By contrast, cells with inducible expression of STAT3 S727A were refractory to TNF+ZVAD-induced necrosis, with 94% of the cells still viable after 18 hours of exposure. Similarly, expression of STAT3 S727A prevented the TNF+ZVAD-induced spike in ROS production, whereas expression of STAT3 Y705A had no inhibitory effect on TNF+ZVAD-induced ROS production (Fig. 2C, right panel).

RIPK-1 activity induces phosphorylation of STAT3 on serine 727 and its translocation to the mito ondria

We next wanted to determine the pathway respo le for the phosphorylation of STAT3 on serine 727 during T ZVAD exposure. During necroptosis, engagem TNF ptor activates RIPK-1. As shown in Fig. 3 siRNAs targeting

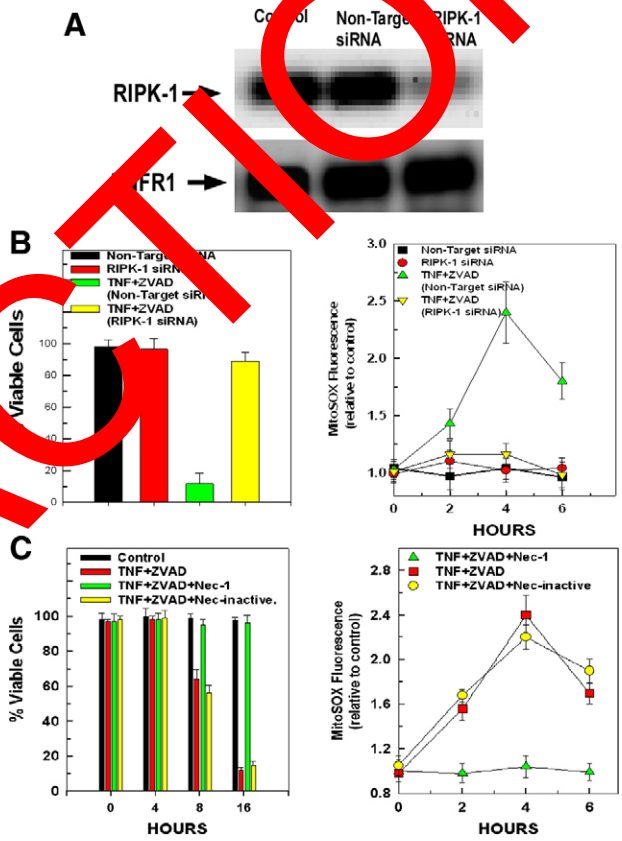

Fig. 3. Suppression of RIPK-1 expression or activity prevents ROS generation and cytotoxicity during TNF-induced necroptosis. (**A**) L929 cells were transfected with 50 nM siRNA targeting RIPK-1 or a non-targeting control siRNA. After incubation for 48 hours, the cells were harvested and the levels of RIPK-1 and TNFR1 were determined by western blotting. The results are representative of three independent experiments. (**B**) L929 cells were transfected with 50 nM siRNA targeting RIPK-1 or a non-targeting control siRNA. After incubation for 48 hours, the cells were incubated with 20 ng/ml TNFα in the presence of 20 μM ZVAD. After 18 hours, the cells were harvested and cell viability assessed using propidium iodide. Alternately, ROS generation was determined at the time points indicated using MitoSOX fluorescence. Values are the means of three independent experiments with the error bars indicating standard deviations. (**C**) Cultured L929 cells were untreated, pretreated with 10 μM necrostatin-1 or the inactive analog of necrostatin-1 (10 μM). After 1 hour, the cells were then exposed to 20 ng/ml TNFα in combination with 20 μM ZVAD. At the time points indicated, the cells were harvested and cell viability and ROS formation were determined using propidium iodide or MitoSOX fluorescence, respectively. Values are the means of three independent experiments with the error bars indicating standard deviations.

RIPK-1 suppressed its expression in L929 cells, but not that of TNFR1. Suppression of RIPK-1 expression prevented both the cytotoxicity and generation of ROS provoked by exposure to TNF+ZVAD. Cells transfected with a non-targeting control siRNA exhibited only 15% viability following 18 hours of exposure to TNF+ZVAD (Fig. 3B, left panel). By contrast, cells transfected with siRNA targeting RIPK-1 displayed a marked resistance to TNF+ZVAD-induced necrosis, with 90% of the cells still viable after 18 hours of TNF+ZVAD treatment (Fig. 3B, left panel). Additionally, suppression of RIPK-1 expression also prevented the antecedent surge of ROS production provoked by exposure to TNF+ZVAD (Fig. 3B, right panel). Necrostatin-1 binds to and inhibits the activity of RIPK-1. As with suppression of RIPK-1 expression, a 1-hour pretreatment with necrostatin-1 prevented the necrosis and surge in ROS production brought about by TNF+ZVAD treatment, whereas an inactive analog of necrostatin, lacking a methyl group, failed to prevent TNF+ZVAD-induced cytotoxicity or ROS generation (Fig. 3C, left and right panels, respectively).

The phosphorylation of STAT3 on serine 727 brought about by TNF+ZVAD exposure for 4 hours was largely prevented by the suppression of RIPK-1 expression (Fig. 4A, lane 3). However, there was slight phosphorylation of STAT3 in cells where RIPK-1 expression was suppressed; despite this, cell death was completely negated, possibly indicating a threshold effect for cell killing. Similarly, pretreatment for 1 hour with necrostatin-1 also prevented the induction of STAT3 phosphorylation on serine 727 brought about by TNF+ZVAD treatment for 4 hours (Fig. 4B, lane 3), whereas pretreatment with the inactive analog of necrostatin-1 failed to inhibit TNF+ZVAD-induced STAT3 phosphorylation (Fig. 4B, lane 4). Importantly, suppression of RIPK-1 or treatment with necrostatin-1 had no effects on total STAT3 expression (Fig. 4A,B).

STAT3 is localized to the mitochondria (Gough et al., 2009; Wegrzyn et al., 2009). Because TNF+ZVAD exposure induced mitochondrial ROS production, we wanted to determine whether TNF+ZVAD had any effect on mitochondrial STAT3 levels. Mitochondria were isolated from L929 cells and mitochondrial lysates probed by western blotting for the levels of STAT3 and serine-727-phosphorylated STAT3. As shown in Fig. 4C (panel 1, lane 1), mitochondria isolated from control cells exhibited a low basal level of STAT3. After 4 hours of TNF+ZVAD exposure, there was a marked accumulation of STAT3 in mitochondrial lysates (Fig. 4C, panel 1, lane 2). Importantly, most of the STAT3 that accumulated in the mitochondria was phosphorylated on serine 727 (Fig. 4C, panel 2, lane 2). Moreover, pretreatment with necrostatin-1 prevented the TNF+ZVAD-induced accumulation of STAT3 in the mitochondria (Fig. 4C, panels 1 and 2, lane 3), whereas the inactive analog of necrostatin-1 did not (Fig. 4C, panels 1 and 2, lane 4). Moreover, as shown in Fig. 5A, lane 4, induction of STAT3 S727A expression prevented TNF+ZVAD-induced phosphorylation of endogenous STAT3, whereas expression of STAT3 Y705A had no effect (Fig. 5A, lane 3). Additionally, as shown in Fig. 5B, lane 2, immunoprecipitation of RIPK-1 revealed that a 2-hour exposure to TNF+ZVAD dramatically increased the interaction between STAT3 and RIPK-1, which was prevented by overexpression of STAT3 S727A (Fig. 5B, lane 4) but was not prevented by STAT3 Y705A (Fig. 5B, lane 3).

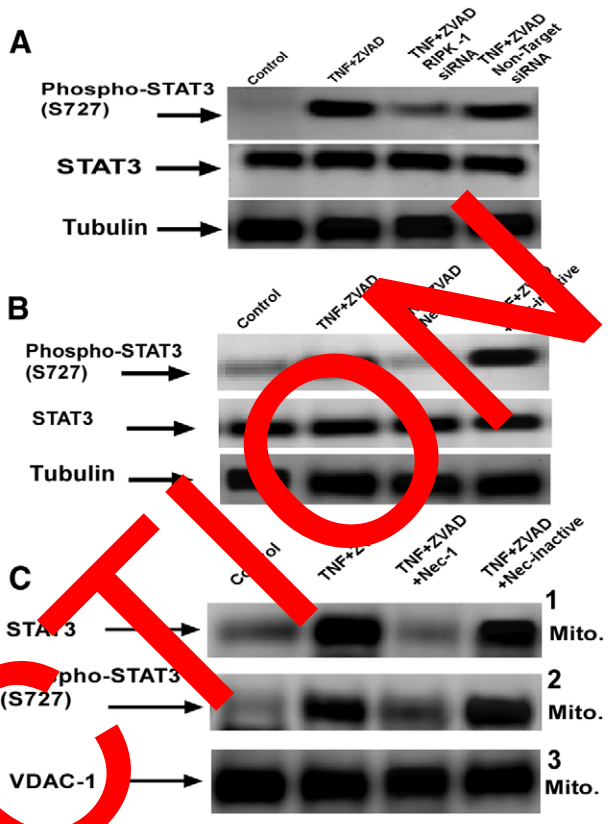

Fig. 4. RIPK-1 activity induces STAT3 phosphorylation on serine 727 and its localization to the mitochondria. (**A**) L929 cells were transfected with 50 nM siRNA targeting RIPK-1 or a non-targeting control siRNA. After 48 hours, the cells were untreated or exposed to 20 ng/ml TNFα in the presence of 20 μM ZVAD. After 4 hours, the cells were harvested. Whole-cell extracts were separated by SDS-PAGE followed by blotting to PVDF membranes. The western blots were developed with an antibody against STAT3 phosphorylated on serine 727. The blots were then stripped and reprobed with antibodies against total STAT3 and tubulin. The results are representative of three independent experiments. (**B**) Cultured L929 cells were untreated, pretreated with 10 μM necrostatin-1 or the inactive necrostatin analog (10 μM). After 1 hour, the cells were exposed to 20 ng/ml TNFα in the presence of 20 μM ZVAD. After 4 hours the cells were harvested. Whole-cell extracts were prepared and separated by SDS-PAGE, followed by blotting to PVDF membranes. The western blots were developed with an antibody against STAT3 phosphorylated on serine 727. The blots were then stripped and reprobed with antibodies against total STAT3 and tubulin. The results are representative of three independent experiments. (**C**) Cultured L929 cells were untreated, pretreated with 10 μM necrostatin-1 or the inactive necrostatin analog (10 μM). After 1 hour, the cells were treated with 20 ng/ml TNFα in the presence of 20 μM ZVAD. After 4 hours exposure, the cells were harvested and mitochondria isolated as described in the Materials and Methods. Mitochondrial extracts were prepared and separated by SDS-PAGE followed by blotting to PVDF membranes. The western blots were developed with antibodies against STAT3 phosphorylated on serine 727. The blots were then stripped and reprobed with an antibody against STAT3, followed by subsequent restripping and probing with an antibody against VDAC-1. The results are representative of three independent experiments.

GRIM-19 mediates the mitochondrial translocation of STAT3 during TNF-induced necroptosis

GRIM-19 is a component of complex I of the mitochondrial respiratory chain and has been implicated in the induction of cell

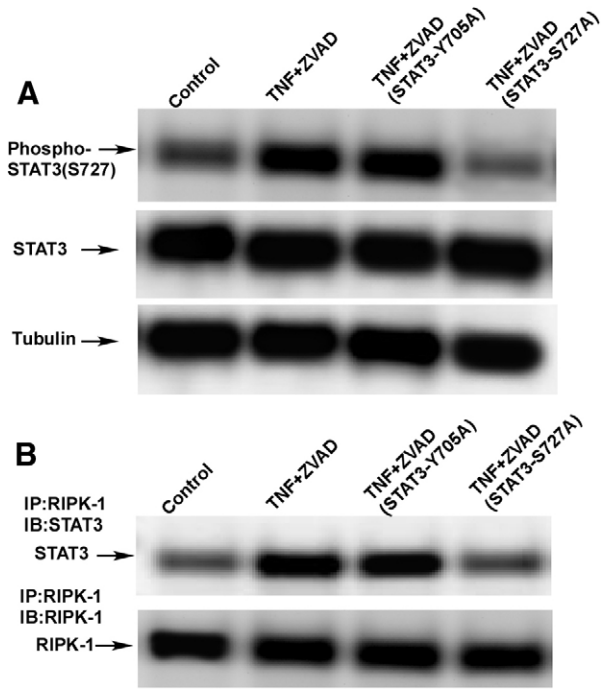

Fig. 5. STAT3 S727A inhibits TNF+ZVAD-induced STAT3 phosphorylation and the interaction of STAT3 with RIPK-1. (**A**) L929 cells were generated for tetracycline-inducible expression of STAT3 S727A or STAT3 Y705A. The cells were plated in 24-well plates at 40,000 cells/well. After 24 hours of induction with 1 μg/ml doxycycline, the cells were treated with 20 ng/ml TNFα in combination with 20 μM ZVAD. After 4 hours the cells were harvested. Whole-cell extracts were prepared and separated by SDS-PAGE, followed by blotting to PVDF membranes. The western blots were developed with an antibody against STAT3 phosphorylated on serine 727. The blots were then stripped and reprobed with antibodies against total STAT3 and tubulin. The results are representative of three independent experiments. (**B**) L929 cells with tetracycline-inducible expression of STAT3 S727A or STAT3Y705A, were plated in 24-well plates at 40,000 cells/well. After 24 hours of induction with 1 μg/ml doxycycline, the cells were treated with 20 ng/ml TNFα in combination with 20 μM ZVAD. After 2 hours the cells were harvested. RIPK-1 was immunoprecipitated from whole-cell extracts. The immunoprecipitates were then separated by SDS-PAGE and blotted onto PVDF membranes. The blots were probed with an antibody against STAT3. The results are representative of three independent experiments.

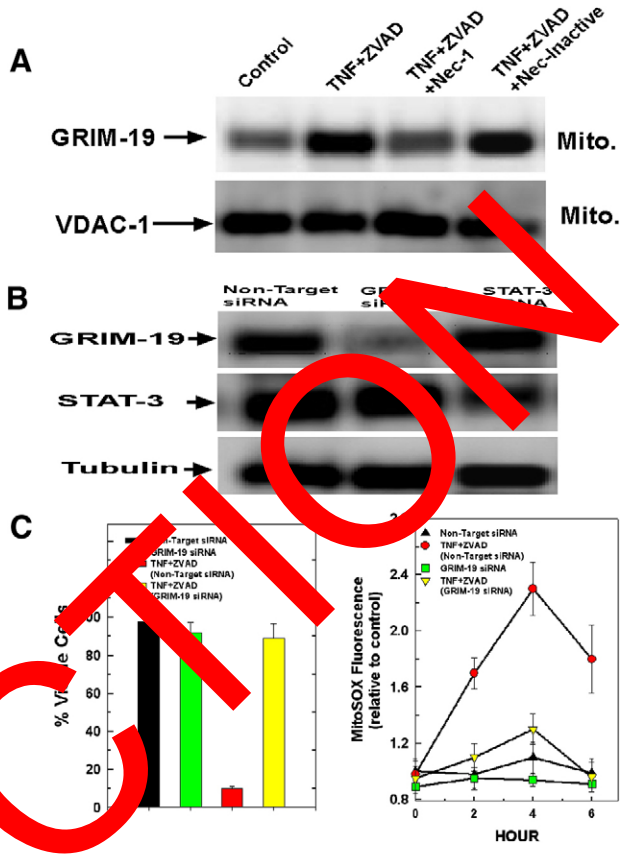

Fig. 6. RIPK-1 activity induces GRIM-19 accumulation in the mitochondria that is required for TNFα-induced necroptosis. (**A**) Cultured L929 cells were untreated, pretreated with 10 μM necrostatin-1 or the inactive necrostatin-1 analog (10 μM). After 1 hour, the cells were exposed to 20 ng/ml TNFα in combination with 20 μM ZVAD. The cells were harvested and mitochondria isolated. Mitochondrial lysates were prepared and separated by SDS-PAGE, followed by blotting onto PVDF membranes. The western blots were then probed with an antibody against GRIM-19, stripped and reprobed with an antibody against VDAC-1. The results are representative of three independent experiments. (**B**) L929 cells were transfected with siRNAs targeting GRIM-19, STAT3 or a non-targeting control siRNA. After 48 hours, the cells were harvested and whole-cell lysates prepared. The lysates were separated by SDS-PAGE gel and blotted onto PVDF membranes. The membranes were probed with antibodies against GRIM-19 or STAT3. The results are representative of three independent experiments. (**C**) L929 cells were transfected with siRNA targeting GRIM-19 or a non-targeting control siRNA. After 48 hours, the cells were treated with 20 ng/ml TNFα in combination with 20 μM ZVAD. After 18 hours, the cells were harvested and cell viability determined using propidium iodide (left graph). Alternatively, the cells were harvested at the times indicated and ROS production measured using MitoSOX fluorescence (right graph). Values are the means of three independent experiments with the error bars indicating standard deviations.

death. Like STAT3, GRIM-19 also localizes to the cytosol, mitochondria and nucleus. Furthermore, GRIM-19 is known to bind to STAT3 with serine 727 being crucial for the interaction. Because STAT3 does not possess a mitochondrial targeting sequence we explored the possibility that GRIM-19 helps to chaperone STAT3 to the mitochondria. As shown in Fig. 6A, lane 1, as expected for a component of mitochondrial complex I, mitochondria isolated from control cells contained a notable level of GRIM-19. However, treatment with TNF+ZVAD for 4 hours caused a striking increase in the level of mitochondrial GRIM-19 (Fig. 6A, lane 2). The stimulation in the level of mitochondrial GRIM-19 brought about by exposure to TNF+ZVAD was dependent on RIPK-1 activity. The RIPK-1 inhibitor, necrostatin-1, prevented the accumulation of mitochondrial GRIM-19 induced by TNF+ZVAD (Fig. 6A, lane 3), whereas the inactive analog of necrostatin-1 failed to prevent the increase of mitochondrial GRIM-19 levels in TNF+ZVAD-treated cells (Fig. 6A, lane 4).

GRIM-19 has been implicated in the induction of ROS generation and cell death. As shown in Fig. 6B, transfection with siRNA targeting GRIM-19 suppressed its expression in L929 cells while having no effect on the levels of STAT3. Similarly, transfection with siRNA targeting STAT3 did not diminish expression of GRIM-19 (Fig. 6B). As shown in Fig. 6C, left panel, suppression of GRIM-19 expression prevented TNF+ZVAD-induced necrosis. In cells transfected with

non-targeting siRNAs, TNF+ZVAD reduced cell viability to 12% following 18 hours of treatment. By contrast, suppression of GRIM-19 levels greatly ameliorated TNF+ZVAD-induced necrosis, with 87% of the cells still viable after 18 hours of exposure to TNF+ZVAD. Similarly, suppression of GRIM-19 expression also prevented the stimulation of ROS production incited by TNF+ZVAD (Fig. 6C, right panel).

Given the known association between STAT3 and GRIM-19, we wanted to determine whether this interaction is modulated during TNF+ZVAD-induced necroptosis. As shown in Fig. 7A, lane 1, immunoprecipitation of GRIM-19 from lysates prepared from mitochondria isolated from control cells detected some interaction between GRIM-19 and STAT3. However, there was a marked stimulation in the interaction of GRIM-19 with STAT3 in lysates prepared from mitochondria isolated after 4 hours of TNF+ZVAD treatment (Fig. 7A, lane 2). Importantly, the enhanced interaction between STAT3 and GRIM-19 induced by TNF+ZVAD was dependent on RIPK-1 activity. Pretreatment with the RIPK-1 inhibitor necrostatin-1, prevented the increased interaction between STAT3 and GRIM-19 brought about by TNF+ZVAD exposure (Fig. 7A, lane 3). By contrast, the stimulation of GRIM-19–STAT3 interaction induced by TNF+ZVAD treatment was not prevented by the inactive necrostatin-1 analog (Fig. 7A, lane 4). We next determined the functional significance of the augmented interaction between GRIM-19 and STAT3 with regards to the increased levels of STAT3 and GRIM-19 in the mitochondria of TNF+ZVAD-treated cells. As shown in Fig. 7B, left panel, suppression of GRIM-19 expression prevented the mitochondrial accumulation of STAT3 upon treatment with TNF+ZVAD. Similarly, suppression of STAT3 levels prevented the accumulation of GRIM-19 in the mitochondria that is triggered by TNF+ZVAD treatment (Fig. 7B, right panel). Interestingly, although suppression of GRIM-19 expression prevented TNF+ZVAD-induced accumulation of STAT3 in the mitochondria, it did not prevent the RIPK-1-dependent phosphorylation of STAT3 in the cytosol (Fig. 7C, lane 3). These data suggest that the interaction between GRIM-19 and STAT3 is required for their mutual translocation to the mitochondria upon TNF+ZVAD exposure for STAT3 phosphorylation.

STAT3 S727D was used to constitutively serine-727-phosphorylated mimetic of STAT3. L929 cells were generated in which the expression of STAT3 S727D was under the control of a tetracycline-inducible promoter. As shown in Fig. 8A, STAT3 S727D expression induced a 62% loss of viability in L929 cells within 48 hours of doxycycline induction, which was not prevented by non-targeting siRNA. However, suppression of GRIM-19 expression prevented the loss of cell viability brought about by STAT3 S727D expression, with 92% of the cells still viable after 48 hours after induction of STAT3 S727D expression with 1 μg/ml doxycycline. These data indicate that GRIM-19 is required for STAT3 S727D to exert a cytotoxic effect (Fig. 8A). As shown in Fig. 8B, lane 2, mitochondria isolated from cells expressing STAT3 S727D exhibited an elevation of GRIM-19 levels in mitochondrial lysates over that of controls (45%

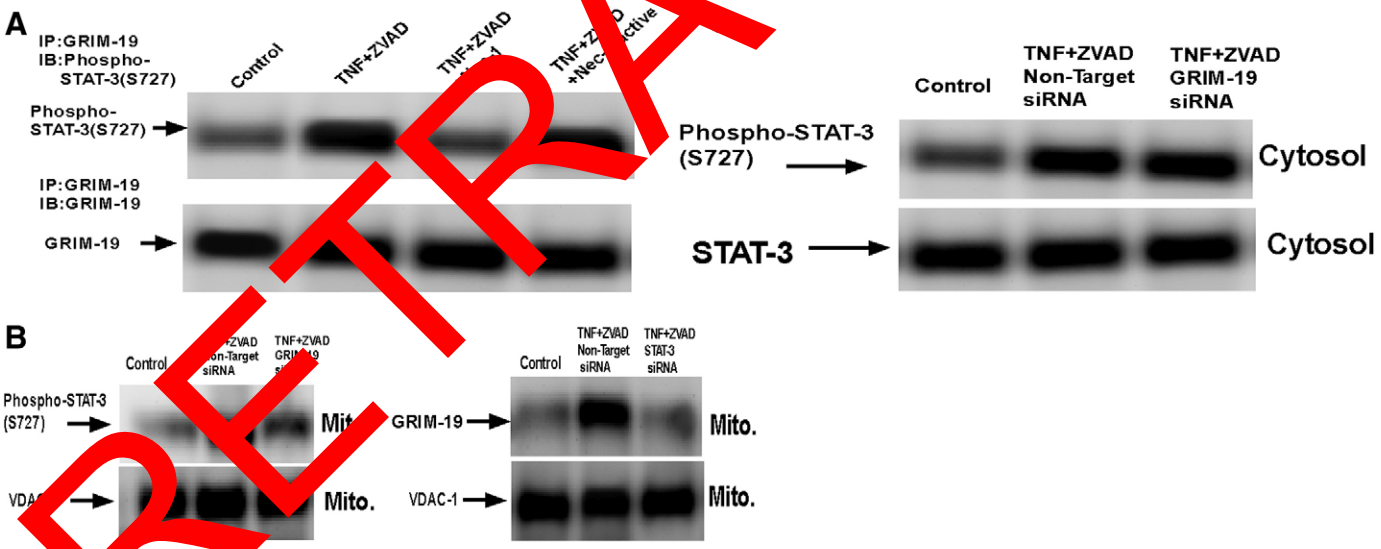

Fig. 7. Interaction between STAT3 and GRIM-19 is required for their translocation to the mitochondria during TNF-induced necroptosis. (**A**) L929 cultures were left untreated or pretreated with 10 μM necrostatin-1 or the inactive necrostatin analog (10 μM). After 1 hour, the cells were exposed to 20 ng/ml TNFα in the presence of 20 μM ZVAD. After 4 hours, the cells were harvested and mitochondria isolated. GRIM-19 was immunoprecipitated from mitochondrial lysates. The immunoprecipitates were then separated by SDS-PAGE and blotted onto PVDF membranes. The blots were probed with an antibody against STAT3 phosphorylated on serine 727. The results are representative of three independent experiments. (**B**) L929 cells were left untreated or transfected with 50 nM siRNA targeting STAT3, GRIM-19 or a non-targeting control siRNA. After 48 hours, the cells were treated with 20 ng/ml TNFα in the presence of 20 μM ZVAD. After 4 hours exposure, the cells were harvested and mitochondria isolated. Mitochondrial lysates were prepared and separated by SDS-PAGE, then blotted onto PVDF membranes. The blots were probed with antibodies directed against GRIM-19 or STAT3 phosphorylated on serine 727. The blots were then stripped and reprobed with an antibody against VDAC-1. The results are representative of three independent experiments. (**C**) L929 cells were transfected with 50 nM siRNA targeting GRIM-19 or a non-targeting control siRNA. After 48 hours, the cells were exposed to 20 ng/ml TNFα in the presence of 20 μM ZVAD. After 4 hours, the cells were harvested and the cytosolic fraction isolated and separated by SDS-PAGE and then blotted onto PVDF membrane. The membranes were then probed with an antibody against STAT3 phosphorylated on serine 727, stripped and reprobed with an antibody against total STAT3. The results are representative of three independent experiments.

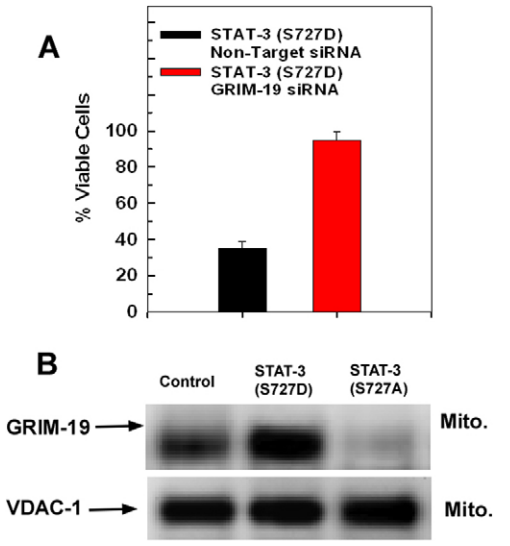

Fig. 8. Expression of a constitutively phosphorylated mimetic of STAT3 induces GRIM-19 translocation to the mitochondria, and cytotoxicity. (**A**) L929 cells were generated that stably expressed a tetracycline-inducible vector for STAT3 S727D. The cells were then either left untreated or transfected with 50 nM siRNA targeting GRIM-19 or a non-targeting control siRNA. Expression of STAT3 S727D was then induced with 1 μg/ml doxycycline. After 48 hours, the cells were harvested and cell viability determined using propiduim iodide. Values are the means of three independent experiments with the error bars indicating standard deviations. (**B**) L929 cells were treated with 1 μg/ml doxycycline to induce the expression of STAT3(S727A) or STAT3(S727D). Following 24 hours, the cells were harvested and mitochondria isolated. Mitochondrial lysates were prepared and separated by SDS-PAGE, then blotted onto PVDF membranes. The blots were probed with an antibody against GRIM-19, then stripped and reprobed with an antibody against VDAC-1. The results are representative of three independent experiments.

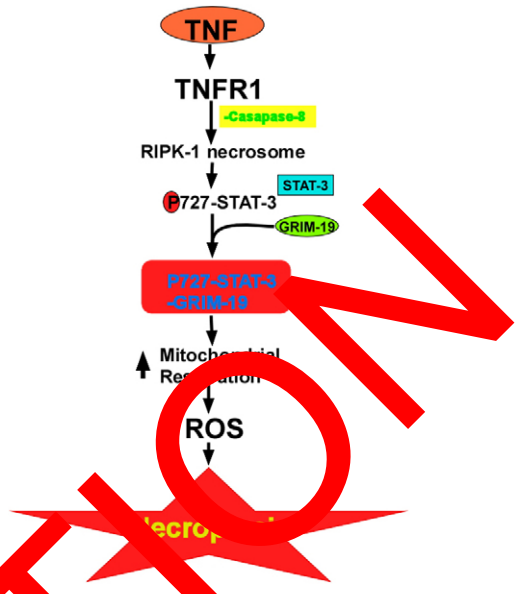

Fig. 9. GRIM-19-[illegible]T3S727A trigger mitochondrial ROS production. TNF-induced necrosome formation triggers phosphorylation of STAT3 on serine 727, which binds to GRIM-19 and induces mitochondrial ROS formation and cytotoxicity by necroptosis.

increase by densitometry), whereas cells [illegible] S727A exhibited a decreased level of GRIM-19 in the mitochondria (Fig. 8B, lane 3, [illegible] decrease by densitometry).

Discussion

The present study presents data indicating that GRIM-19 and STAT3 are crucial components of the TNF-induced necroptosis pathway. STAT3 is phosphorylated on serine 727 when the TNF receptor is engaged in the absence of caspase activation. The phosphorylation of STAT3 is dependent on RIPK-1 expression and activity. The phosphorylation of STAT3 on serine 727 increases its interaction with GRIM-19, leading to their accumulation in the mitochondria where they incite an increase in ROS generation resulting in cell death by necroptosis (Fig. 9).

STAT3 is a transcription factor stimulated by the interleukin-6 family of cytokines and growth factors. In the nucleus, STAT3 induces the expression of a number of genes crucial for cell survival and growth (Bernier et al., 2011; Demaria et al., 2010; Demaria and Poli, 2011). In tumor cells, STAT3 phosphorylation on tyrosine 705 induces dimerization and nuclear localization. However, recent reports also indicate a mitochondrial localization for STAT3. In the mitochondria, STAT3 seems to be necessary for optimal functioning of the mitochondrial respiratory chain (Bernier et al., 2011; Qiu et al., 2011). Mitochondria isolated from cardiomyocytes of *Stat3*$^{-/-}$ mice showed a decrease of complex I and II activities (Wegrzyn et al., 2009). Moreover, expression of STAT3 targeted exclusively to the mitochondria restored mitochondrial respiration. Similarly, Ras-dependent transformation was reconstituted in *Stat3*$^{-/-}$ cells with STAT3 mutants that were transcriptionally inactive by mutation of tyrosine 705 but able to localize to mitochondria (Gough et al., 2009). By contrast, mutation of serine 727 to alanine negated the ability of STAT3 to restore Ras-dependent transformation and mitochondrial activity, whereas substitution with the phosphorylation mimetic, STAT3 S727D, enhanced both Ras transformation and mitochondrial function. Similarly, in neuronal cells, nerve growth factor (NGF) induced phosphorylation of STAT3 on serine 727, resulting in an increased mitochondrial localization of STAT3 and elevation of mitochondrial ROS production, both necessary for NGF-stimulated neurite outgrowth (Zhou and Too, 2011). It has also been demonstrated that STAT3 targeted to the mitochondria protects against ischemia-induced changes in the activity of mitochondrial complex I and II and binds to cyclophilin-D (Boengler et al., 2010; Szczepanek et al., 2011). How mitochondrial STAT3 induces alterations of mitochondrial function is unclear, because a recent study indicated that, under basal conditions, STAT3 is not present in the mitochondria sufficiently to interact stoichiometrically with components of complex I or II (Phillips et al., 2010).

Similar to STAT3, GRIM-19 is also found in many cellular compartments, with localization being modified by cytokines and growth factors. GRIM-19 is a component of complex I of the mitochondrial respiratory chain and is required for maintenance of mitochondrial membrane potential (Fearnley et al., 2001; Lu and Cao, 2008). GRIM-19 binds to and suppresses the transcriptional activity of STAT3, with serine 727 being required for the STAT3–GRIM-19 interaction (Lufei et al., 2003; Nallar et al., 2010; Zhang et al., 2003). GRIM-19 is selective for STAT3 and is not known to bind the other STAT family members. By binding to nuclear STAT3, GRIM-19

suppresses the expression of proteins required for cell metabolism, cell cycle progression and the Bcl-2 family of anti-apoptotic proteins, leaving the cell vulnerable to injury. In this way GRIM-19 behaves as a tumor suppressor (Kalakonda et al., 2007; Okamoto et al., 2010; Wang et al., 2011). Moreover, there is evidence that the mitochondrial localization of GRIM-19 in and of itself enhances cytokine-induced cytotoxicity. Interferon-β in combination with retinoic acid potently induces cellular demise through a ROS-dependent mechanism. Indeed, treatment with interferon-β and retinoic acid induces an increase in GRIM-19 in the mitochondria that colocalizes with elevated levels of STAT3. Lowering GRIM-19 levels ameliorated interferon-β–retinoic-acid-induced cell death and ROS generation (Huang et al., 2007). Interestingly a 2.7 kb virally encoded RNA from human cytomegalovirus binds to GRIM-19 and inhibits cytokine-induced cell death by preventing GRIM-19 accumulation in the mitochondria (Reeves et al., 2007). Such observations indicate that GRIM-19 has dual functions that work in tandem in mediating cell injury. In the nucleus, GRIM-19 binds to STAT3 and suppresses expression of proteins that enhance cell survival, whereas in the mitochondria, GRIM-19 induces ROS generation, resulting in cell injury and death.

The RIPK-1–RIPK-3 necrosome activates enzymes involved in energy metabolism, such as glutamate dehydrogenase and glycogen phosphorylase (Zhang et al., 2009). The activation of such metabolic enzymes would feed substrates into the Krebs cycle, producing NADH that stimulates mitochondrial respiratory chain activity. The phosphorylation of STAT3 and its accumulation in the mitochondria with GRIM-19 would further enhance mitochondrial respiration. In some instances, the stimulation of respiratory activity triggered by mitochondrial STAT3 is protective, especially against ischemic damage (Szczepanek et al., 2011). So by an uncharacterized mechanism, during the induction of necroptosis, the physiological and protective response of increased mitochondrial respiration induced by STAT3 undergoes metamorphosis into a damaging event. Presently, the data demonstrate that RIPK-1 expression and activity are required for phosphorylation of STAT3 during TNF-induced necroptosis, but do not definitively identify RIPK-1 as the kinase responsible for the phosphorylation of STAT3. It is conceivable that RIPK-1 activates downstream kinases that in turn phosphorylate STAT3. Indeed, STAT3 is phosphorylated on serine 727 by a number of kinases including mTOR that do not necessarily result in necroptosis (Ge and Ren, 2012; Yokogami et al., 2000; Yokoya et al., 2007). Whether phosphorylation of STAT3 at serine 727 influences its interaction with GRIM-19 and their mitochondrial relocalization in other cellular contexts is unknown. The degree to which GRIM-19 and STAT3 accumulate in the mitochondria could influence the cells fate. Currently, however, the mechanism(s) that regulate the influx and egress of GRIM-19 and STAT3 to and from mitochondria is not characterized.

Materials and Methods

Cell culture

L929 mouse fibrosarcoma cells were maintained in Dulbecco's modified Eagle's medium containing 10% fetal bovine serum, 100 units/ml penicillin and 100 μg/ml streptomycin under an atmosphere of 95% air and 5% CO_2 at 37℃. Cells were subcultured 1:5 once a week.

Treatments and transfection with siRNAs

L929 cells were plated in either 24-well plates at 50,000 cells/well or in 25 cm^2 flask at 1.0×10^6 cells. Following overnight incubation, cells were treated with 20 ng/ml TNFα (Santa Cruz Biotechnology) in the presence or absence of 20 μM Z-VAD-FMK (Santa Cruz Biotechnology). Where indicated, L929 cells were transfected with the indicated siRNAs targeting STAT3, STAT1, GRIM-19 or with a non-targeting control siRNA using a lipid-based method supplied from a commercial vendor (Gene Therapy Systems, San Diego, CA) at a final siRNA concentration of 50 nM. After formation of the siRNA–liposome complexes, the mixture was added to the L929 cells for 24 hours. Afterward, the medium was aspirated, and complete medium was added back for a further 24 hours, after which time the cells were used for experiments. Tetracycline-inducible L929 cells were generated using the Tet-ON/Tet-Off system (Promega). Where indicated, expression of STAT3 mutants was induced by incubating with 1 μg/ml doxycycline. Expression of STAT3 mutants was maximal after 24 hours after doxycycline addition, at which time, where indicated, the cells were treated with TNF and ZVAD.

Measurements of cell viability and ROS

Following treatments, L929 cells were harvested and centrifuged at 700 ***g***. The cell pellet was resuspended in phosphate buffered saline to which was added 5 μM propidium iodide. After 5 minutes incubation, cells were pelleted and resuspended in PBS. The percentage of viable cells was determined, using a Cellometer (Nexelom, Lawrence, MA), as the ratio of the number of cells in the fluorescent images (propidium iodide positive) to the bright-field images. For measurement of ROS production, 5 μM MitoSOX (Invitrogen) was added to cells 10 minutes before harvesting. The cells were pelleted and resuspended in PBS. In cells with active production of ROS, MitoSOX oxidized to a fluorescent species. The percentage MitoSOX-positive cells was determined using a Cellometer, which calculated the ratio of the number of MitoSOX-positive cells in the fluorescence images to the number of cells in the bright-field images.

Isolation of mitochondrial and cytosolic fractions

Following treatments, approximately 1.0×10^6 cells from a 25 cm^2 flask were harvested by trypsinization and centrifuged at 700 ***g*** for 10 minutes at 4℃ as described previously (Shulga et al., 2010). The cell pellets were washed once in PBS and then resuspended in 3 volumes of isolation buffer (20 mM Hepes, pH 7.4, 10 mM KCl, 1.5 mM $MgCl_2$, 1 mM sodium EDTA, 1 mM dithiothreitol, 10 mM phenylmethylsulfonyl fluoride, 10 μM leupeptin and 10 μM aprotinin) in 250 mM sucrose. After swelling on ice for 3 minutes, the cells were disrupted by 40 strokes of a glass homogenizer. The homogenate was centrifuged twice at 1500 ***g*** at 4℃ to remove unbroken cells and nuclei. The mitochondria-enriched fraction (heavy membrane fraction) was then pelleted by centrifugation at 12,000 ***g*** for 30 minutes. The supernatant was removed and then filtered through a 0.2 μm and then a 0.1 μm Ultrafree-MC filter to obtain the cytosolic fraction.

Immunoprecipitation of GRIM-19 and RIPK-1

GRIM-19 or RIPK-1 was immunoprecipitated from mitochondrial extracts or whole-cell extracts, respectively (GRIM-19 antibody from Novus Biologicals and RIPK-1 antibody from Cell Signaling). The immunoprecipitates were then run on SDS-PAGE gels and blotted onto PVDF membranes. The western blots were developed with antibodies against STAT3 phosphorylated on serine 727 (Cell Signaling).

Statistical analysis

Results are expressed as means ± s.d. of at least three independent experiments. Statistical significance was defined at $P<0.05$.

Funding

This work was supported in part by the National Cancer Institute [grant number 5R01AA012897-11]; and the National Institute of Alcohol Abuse and Alcoholism [grant number 5R01CA118356-07].

Supplementary material available online at
http://jcs.biologists.org/lookup/suppl/doi:10.1242/jcs.103093/-/DC1

References

Bernier, M., Paul, R. K., Martin-Montalvo, A., Scheibye-Knudsen, M., Song, S., He, H. J., Armour, S. M., Hubbard, B. P., Bohr, V. A., Wang, L. et al. (2011). Negative regulation of STAT3 protein-mediated cellular respiration by SIRT1 protein. *J. Biol. Chem.* **286**, 19270-19279.

Boengler, K., Hilfiker-Kleiner, D., Heusch, G. and Schulz, R. (2010). Inhibition of permeability transition pore opening by mitochondrial STAT3 and its role in myocardial ischemia/reperfusion. *Basic Res. Cardiol.* **105**, 771-785.

Cho, Y. S., Challa, S., Moquin, D., Genga, R., Ray, T. D., Guildford, M. and Chan, F. K. (2009). Phosphorylation-driven assembly of the RIP1-RIP3 complex regulates programmed necrosis and virus-induced inflammation. *Cell* **137**, 1112-1123.

Demaria, M. and Poli, V. (2011). From the nucleus to the mitochondria and back: The odyssey of a multitask STAT3. *Cell Cycle* **10**, 3221-3222.

Demaria, M., Giorgi, C., Lebiedzinska, M., Esposito, G., D'Angeli, L., Bartoli, A., Gough, D. J., Turkson, J., Levy, D. E., Watson, C. J. et al. (2010). A STAT3-mediated metabolic switch is involved in tumour transformation and STAT3 addiction. *Aging (Albany NY)* **2**, 823-842.

Fearnley, I. M., Carroll, J., Shannon, R. J., Runswick, M. J., Walker, J. E. and Hirst, J. (2001). GRIM-19, a cell death regulatory gene product, is a subunit of bovine mitochondrial NADH:ubiquinone oxidoreductase (complex I). *J. Biol. Chem.* **276**, 38345-38348.

Galluzzi, L., Vanden Berghe, T., Vanlangenakker, N., Buettner, S., Eisenberg, T., Vandenabeele, P., Madeo, F. and Kroemer, G. (2011). Programmed necrosis from molecules to health and disease. *Int. Rev. Cell Mol. Biol.* **289**, 1-35.

Ganten, T. M., Haas, T. L., Sykora, J., Stahl, H., Sprick, M. R., Fas, S. C., Krueger, A., Weigand, M. A., Grosse-Wilde, A., Stremmel, W. et al. (2004). Enhanced caspase-8 recruitment to and activation at the DISC is critical for sensitisation of human hepatocellular carcinoma cells to TRAIL-induced apoptosis by chemotherapeutic drugs. *Cell Death Differ.* **11 Suppl. 1**, S86-S96.

Ge, W. and Ren, J. (2012). mTOR-STAT3-notch signaling contributes to ALDH2-induced protection against cardiac contractile dysfunction and autophagy under alcoholism. *J. Cell Mol. Med.* **16**, 616-626.

Goossens, V., Grooten, J., De Vos, K. and Fiers, W. (1995). Direct evidence for tumor necrosis factor-induced mitochondrial reactive oxygen intermediates and their involvement in cytotoxicity. *Proc. Natl. Acad. Sci. USA* **92**, 8115-8119.

Gough, D. J., Corlett, A., Schlessinger, K., Wegrzyn, J., Larner, A. C. and Levy, D. E. (2009). Mitochondrial STAT3 supports Ras-dependent oncogenic transformation. *Science* **324**, 1713-1716.

Huang, G., Chen, Y., Lu, H. and Cao, X. (2007). Coupling mitochondrial respiratory chain to cell death: an essential role of mitochondrial complex I in the interferon-beta and retinoic acid-induced cancer cell death. *Cell Death Differ.* **14**, 327-337.

Kalakonda, S., Nallar, S. C., Lindner, D. J., Hu, J., Reddy, S. P. and Kalvakolanu, D. V. (2007). Tumor-suppressive activity of the cell death activator GRIM-19 on a constitutively active signal transducer and activator of transcription 3. *Cancer Res.* **67**, 6212-6220.

Kasof, G. M., Prosser, J. C., Liu, D., Lorenzi, M. V. and Gomes, B. C. (2000). The RIP-like kinase, RIP3, induces apoptosis and NF-kappaB nuclear translocation and localizes to mitochondria. *FEBS Lett.* **473**, 285-291.

Kim, J. W., Choi, E. J. and Joe, C. O. (2000). Activation of death-inducing signaling complex (DISC) by pro-apoptotic C-terminal fragment of RIP. *Oncogene* **19**, 4491-4499.

Kuwana, T., Smith, J. J., Muzio, M., Dixit, V., Newmeyer, D. D. and Kornbluth, S. (1998). Apoptosis induction by caspase-8 is amplified through the mi[illegible]drial release of cytochrome c. *J. Biol. Chem.* **273**, 16589-16594.

Lin, Y., Choksi, S., Shen, H. M., Yang, Q. F., Hur, G. M., Kim, Y. S., Tra[illegible] J. H., Nedospasov, S. A. and Liu, Z. G. (2004). Tumor necrosis factor-[illegible]uced nonapoptotic cell death requires receptor-interacting protein-mediated c[illegible]ular reactive oxygen species accumulation. *J. Biol. Chem.* **279**, [illegible]828.

Lu, H. and Cao, X. (2008). GRIM-19 is essential for ma[illegible]enance [illegible]mitochon[illegible]l membrane potential. *Mol. Biol. Cell* **19**, 1893-1902.

Lufei, C., Ma, J., Huang, G., Zhang, T., Novotny-Die[illegible]vr, V., Ong [illegible]T. and Cao, X. (2003). GRIM-19, a death-regulatory gene produc[illegible]uppresse[illegible]ia functional interaction. *EMBO J.* **22**, 1325-133[illegible]

Nallar, S. C., Kalakonda, S., Sun, P., Ohmo[illegible], Hiroi, M[illegible]ori, K., Lindner, D. J. and Kalvakolanu, D. V. (2010). Ident[illegible]tion of a structu[illegible]motif in the tumor-suppressive protein GRIM-19 require[illegible]ntitumor activity. *J. Pathol.* **177**, 896-907.

Oberst, A., Dillon, C. P., Weinlich, R., McCorm[illegible]L. L., Fitzgerald, P., Pop, C., Hakem, R., Salvesen, G. S[illegible]nd Green, D. R. [illegible]11). Catalytic activity of the caspase-8-FLIP(L) compl[illegible]nhibits RIPK3-depende[illegible]ecrosis. *Nature* **471**, 363-367.

Okamoto, T., Inozum[illegible], Mitsui, H[illegible]anzaki, M., Harada, K., Shibagaki, N. and Shimada, S. (2010)[illegible]erexpres[illegible]of GRIM-19 in cancer cells suppresses STAT3-mediated signal transd[illegible]n [illegible]cancer grow[illegible]. *Mol. Cancer Ther.* **9**, 2333-2343.

Phillips, D., Reilley, M. J., Aponte, A. M., Wang, G., Boja, E., Gucek, M. and Balaban, R. S. (2010). Stoichiometry of STAT3 and mitochondrial proteins: Implications for the regulation of oxidative phosphorylation by protein-protein interactions. *J. Biol. Chem.* **285**, 23532-23536.

Qiu, H., Lizano, P., Laure, L., Sui, X., Rashed, E., Park, J. Y., Hong, C., Gao, S., Holle, E., Morin, D. et al. (2011). H11 kinase/heat shock protein 22 deletion impairs both nuclear and mitochondrial functions of STAT3 and accelerates the transition into heart failure on cardiac overload. *Circulation* **124**, 406-415.

Reeves, M. B., Davies, A. A., McSharry, B. P., Wilkinson, G. W. and Sinclair, J. H. (2007). Complex I binding by a virally encoded RNA regulates [illegible]itochondria-induced cell death. *Science* **316**, 1345-1348.

Schulze-Osthoff, K., Bakker, A. C., Vanhaesebroeck, B., Beyaert[illegible] Jacob, W. A. and Fiers, W. (1992). Cytotoxic activity of tumor necrosis factor is [illegible]ated by early damage of mitochondrial functions. Evidence for the involvement of [illegible]chondrial radical generation. *J. Biol. Chem.* **267**, 5317-5323[illegible]

Shulga, N., Wilson-Smith, R. and Pastorino, J. G. (2[illegible]Sirtuin[illegible]n of cyclophilin D induces dissociation of hexokinase II fr[illegible]he mitochondria. *J. Cell Sci.* **123**, 894-902.

Szczepanek, K., Chen, Q., Derecka, [illegible], Salloum[illegible]N., Z[illegible]g, Q., Szelag, M., Cichy, J., Kukreja, R. C., Dulak, [illegible], Lesnefsky, E.[illegible]al. (2[illegible]Mitochondrial-targeted Signal transducer and act[illegible]tor of transcriptio[illegible](STAT3) protects against ischemia-induced changes in the [illegible]ectron transport c[illegible]n and the generation of reactive oxygen species. *J. Biol. C[illegible]n.* **286**, 29610-296[illegible]

Vandenabeele, P., Decle[illegible]W., V[illegible]Herreweghe, [illegible]and Vanden Berghe, T. (2010). The role of the kin[illegible]RIP1 a[illegible]RIP3 in TN[illegible]nduced necrosis. *Sci. Signal.* **3**, re4.

Vanlangenakker[illegible], Vanden Be[illegible]e, T., Bogaert, P., Laukens, B., Zobel, K., Deshayes, K[illegible]cic, D., Fulda, S.[illegible]ndenabeele, P. and Bertrand, M. J. (2011). cIAP1 and [illegible]tect cells from T[illegible]nduced necrosis by preventing RIP1/RIP3-depend[illegible]reactive[illegible]gen species production. *Cell Death Differ.* **18**, 656-665.

Vercammen, D., Beyaer[illegible], Denecker, G., Goossens, V., Van Loo, G., Declercq, W., Grooten, J., Fiers, W. a[illegible]Vandenabeele, P. (1998). Inhibition of caspases increases [illegible]tivity of L929 cells[illegible]ecrosis mediated by tumor necrosis factor. *J. Exp. Med.* **187**, 1477-1485.

Wallach, D., Kovalenko, A. and Kang, T. B. (2011). 'Necrosome'-induced inflammation: [illegible]t cells die for it? *Trends Immunol.* **32**, 505-509.

Wang, T., Yan, X[illegible], Zhao, J. J., Ye, J., Jiang, Z. F., Wu, D. R., Xiao, W. H. and Liu, R. Y. (20[illegible]). Gene associated with retinoid-interferon-induced mortality-19 [illegible]ppresses gr[illegible]n of lung adenocarcinoma tumor in vitro and in vivo. *Lung Cancer* [illegible]

Wegrzyn, J., Potla, R., Chwae, Y. J., Sepuri, N. B., Zhang, Q., Koeck, T., Derecka, M., Szczepanek, K., Szelag, M., Gornicka, A. et al. (2009). Function of mitochondrial [illegible]in cellular respiration. *Science* **323**, 793-797.

Yokogami, K., Wakisaka, S., Avruch, J. and Reeves, S. A. (2000). Serine phosphorylation and maximal activation of STAT3 during CNTF signaling is mediated by the rapamycin target mTOR. *Curr. Biol.* **10**, 47-50.

Yokoyama, T., Kondo, Y. and Kondo, S. (2007). Roles of mTOR and STAT3 in autophagy induced by telomere 3′ overhang-specific DNA oligonucleotides. *Autophagy* **3**, 496-498.

Zhang, D. W., Shao, J., Lin, J., Zhang, N., Lu, B. J., Lin, S. C., Dong, M. Q. and Han, J. (2009). RIP3, an energy metabolism regulator that switches TNF-induced cell death from apoptosis to necrosis. *Science* **325**, 332-336.

Zhang, J., Yang, J., Roy, S. K., Tininini, S., Hu, J., Bromberg, J. F., Poli, V., Stark, G. R. and Kalvakolanu, D. V. (2003). The cell death regulator GRIM-19 is an inhibitor of signal transducer and activator of transcription 3. *Proc. Natl. Acad. Sci. USA* **100**, 9342-9347.

Zhou, L. and Too, H. P. (2011). Mitochondrial localized STAT3 is involved in NGF induced neurite outgrowth. *PLoS ONE* **6**, e21680.

Zhuang, S., Lynch, M. C. and Kochevar, I. E. (1999). Caspase-8 mediates caspase-3 activation and cytochrome c release during singlet oxygen-induced apoptosis of HL-60 cells. *Exp. Cell Res.* **250**, 203-212.